gine. Studies with highly purified rat CRF in a bioassay and several radioimmunoassays indicate that CRF antiserum C-30 may have less than 30 times the affinity for rat CRF than it has for ovine CRF.
8. CRF was synthesized (*3*) and dissolved in a mixture of 0.1 percent bovine serum albumin and 0.1 percent ascorbic acid and saline.
9. ACTH was measured by radioimmunoassay (*4*), with sheep antiserum to ACTH. The minimum detectable amount of ACTH was 50 pg/ml.
10. B. Nichols and R. Guillemin, *Endocrinology* **64**, 914 (1959); B. L. Nichols, *Yale J. Biol. Med.* **33**, 415 (1961); A. V. Schally, A. Arimura, C. Y. Bowers, A. J. Kastin, S. Sawano, T. W. Redding, *Recent Prog. Horm. Res.* **24**, 497 (1968); J. C. Buckingham, *Pharmacol. Rev.* **31**, 253 (1980); G. Gillies, T. B. Van Wimersma Greidanus, P. J. Lowry, *Endocrinology* **103**, 528 (1978).
11. J. C. Buckingham and J. H. Leach, *J. Physiol. (London)* **296**, 87P (1979); G. Gillies and P. Lowry, *Nature (London)* **278**, 463 (1979).
12. W. Vale, C. Rivier, J. Spiess, M. Brown, J. Rivier, in *Brain Peptides*, D. Krieger *et al.*, Eds. (Wiley, New York, in press).
13. Supported in part by NIH grants AM26741, AM20917, AM18811, AA03504, and HD13527; by the Rockefeller Foundation; and by the March of Dimes Birth Defects Foundation. Research conducted in part by the Clayton Foundation for Research, California division. C.R. and W.V. are Clayton Foundation investigators. We thank M. Tam, N. Keating, S. Quijada, P. Hernandez, R. Kaiser, R. Galyean, M. Newbury, R. McClintock, G. Yamamoto, J. Vaughan, and C. Douglas for technical assistance and L. Wheatley and S. McCall for manuscript preparation. We are also indebted to D. Orth for providing the antiserum to ACTH.

19 May 1982; revised 9 August 1982

Direct Measurement of Pulmonary Capillary Transit Times

Abstract. *Direct measurements of capillary transit times in dog lungs were made by using in vivo television microscopy. Mean transit times were unexpectedly long. As pulmonary artery pressures were raised, transit times decreased, suggesting that the normally existing hydrostatic pressure gradient in the lung causes a vertical distribution of transit times. The more rapid transit times approached the minimum time required for complete oxygenation.*

The time that blood spends in the pulmonary capillaries is a major determinant of the effectiveness of the gas exchange in the lung. Complete oxygenation occurs in a remarkably short time. Red cells spend about 0.75 second in the pulmonary capillaries in resting subjects and only 0.3 second during exercise (*1, 2*). These values, however, are based on indirect measures of mean capillary transit times for the lung as a whole. They provide no information about the range of transit times in individual capillary beds, in different hydrostatic zones of the lung, or during altered hemodynamic states. The most rapid transit times are especially important, for if some red cells pass through the gas-exchange vessels too quickly, arterial hypoxemia can result. Very rapid red cell transit may be involved in the exercise-induced arterial hypoxemia found in patients with restricted pulmonary vascular beds, in normal individuals (*3, 4*), and even some world-class runners (*5*). To confirm the indirect estimates of mean pulmonary capillary transit times and to determine the range of transit times, we made direct measurements of the passage of blood across single pulmonary capillary networks by using television microscopy in vivo.

Eight pentobarbital-anesthetized dogs (mean weight, 24 kg) were prepared for measurement of systemic and pulmonary arterial pressures, blood gases, and cardiac output (*6*). These measurements were in the normal range. A transparent window was then implanted in the ninth left intercostal space to permit alveolar capillaries on the surface of the left lower lobe to be studied (*7, 8*). The animals were placed in the right lateral decubitus position so that the microscope looked down through the window at the uppermost surface of the lung. To determine capillary transit time a fluorescent dye, fluorescein isothiocyanate in dextran (*9*), was injected through a catheter placed in the left lower lobe artery under fluoroscopic guidance (*10*). Passage of the dye through the microcirculation was observed with a Leitz Ultropak microscope coupled to a COHU 4400 television camera and was recorded on videotape with a Panasonic PV-1210 video (VHS) recorder. To measure capillary transit time, it was necessary to determine when an average molecule in the dye bolus entered and exited a single capillary bed. As the videotape was replayed, the dye passage through the arteriole (diameter, < 20 μm) and a small venule (< 15 μm) serving a common capillary network was electronically sampled. The signals were passed through a sample-and-hold circuit at 60 Hz and then recorded oscillographically to produce dye dilution curves (Fig. 1). A signal indicating the time of dye injection was placed on the audio channel of the videotape and later transcribed with the dye dilution curves. The time at which the average molecule passed the sample window was determined by calculating the first moment (time-weighted mean) of each curve. Mean capillary transit time was obtained by subtracting the first moments of the arteriolar and venular curves with reference to the common injection time signal.

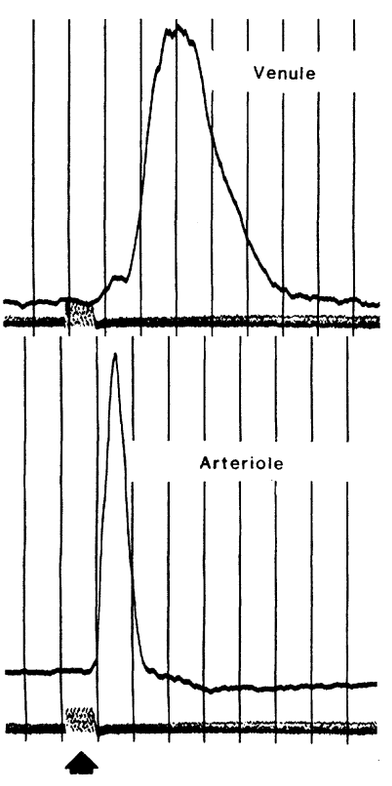

Fig. 1. Photometric records of passage of fluorescein isothiocyanate through a venule and an arteriole. Time lines represent individual seconds. The venular curves were consistently wider than the arteriolar curves, indicating that some of the dye was delayed in its passage through the capillary bed—that is, that there was a distribution of transit times in the capillary bed.

The average of the mean capillary transit times for eight dogs under control conditions was 12.7 ± 3.2 seconds (mean $\pm$ standard error) at an average pulmonary artery pressure of 7.7 ± 1.0 torr (*11*). This transit time was unexpectedly long—more than an order of magnitude longer than the 0.75 second for whole lung capillary transit found by indirect techniques. In fact, the mean capillary transit time we measured is even longer than the mean transit time across the whole lung; mean transit time from the main pulmonary artery to the left atrium was shown by Maseri *et al.* (*12*) to be 6.4 seconds and by Knopp and Bassingthwaighte (*13*) to be 6.8 seconds.

The differences between our measurements and those made with other techniques may be explained by the observation that plasma travels across the lung more slowly than red cells (*14*). Fluorescein isothiocyanate in dextran labels

0036-8075/82/1022-0379$01.00/0

plasma. Through the whole lung, however, plasma travels only 10 percent slower than red cells (*15*), an insufficient difference to account for our long transit times.

Another explanation for our long transit times is that blood flow through subpleural capillaries may not be representative of flow through internal capillary networks. This possibility cannot be examined directly because of the inaccessibility of internal capillary networks. However, an extensive theoretical analysis by Overholser *et al.* (*16*) suggests that, although morphological differences exist between subpleural and internal capillary beds, they do not cause important hemodynamic differences between the two regions. Thus it is probable that our measurements for subpleural vessels reflect transit times in the internal capillaries in the same hydrostatic zone.

The most likely explanation for our long transit times is low driving pressures at the location of the window over the upper lung, where blood flow is low (*17*). If this explanation is correct, then greater driving pressure should reduce transit times. We tested this idea by increasing pulmonary artery pressure with isocapnic hypoxia. As pulmonary artery pressure rose, mean transit time decreased (Fig. 2A). At pressures above 10 torr, mean transit times averaged 4.0 seconds. Because there is a vertical distribution of arterial pressures in the lung (*17*), our data suggest that there is also a vertical distribution of transit times in the lung, with the shortest times in the lower lung, where blood flow is high.

To determine by another method whether there is a large vertical distribution of flow velocities, we measured the clearance rate of angiographic material injected into large arteries (diameter, >3 mm) at two hydrostatic levels in the lung. In four pentobarbital-anesthetized dogs we passed an arterial catheter into the periphery of the left lower lobe, injected contrast material (Hypaque; Winthrop), videotaped the fluoroscopic arteriogram, and measured the time required for clearance of the dye signal from the arteries using our television photometer system. By keeping the catheter in the same artery and rotating the dog from the left to the right lateral decubitus position, we could compare washout times of arteriograms in the lower and upper position. Washout time was three times longer in the upper position. Thus, with an independent method, we found a large difference in blood flow velocity between two different hydrostatic levels in the lung. These data support our idea of a vertical distribution of transit times.

We estimated the shortest transit times to determine whether they approach the minimum time required for complete red cell oxygenation. The most rapid transits were estimated by subtracting the beginning of the arteriolar curve from the beginning of the venular curve. Even under the relatively sluggish flow conditions of the upper lung, the shortest time (0.3 second) approached what is considered to be the lower limit (0.25 second) (*18*) for adequate exposure to alveolar gas. If this is the case in the upper lung, it seems possible that many red cells in the lower lung, even under resting conditions, traverse the capillaries too rapidly for complete oxygenation. However, oxygenation is complete during rest. It may be that the red cells that are still desaturated after leaving the capillaries continue taking up oxygen in the venules. There is evidence that red cell oxygenation begins in arterioles (*19*); oxygen uptake could continue in venules as well.

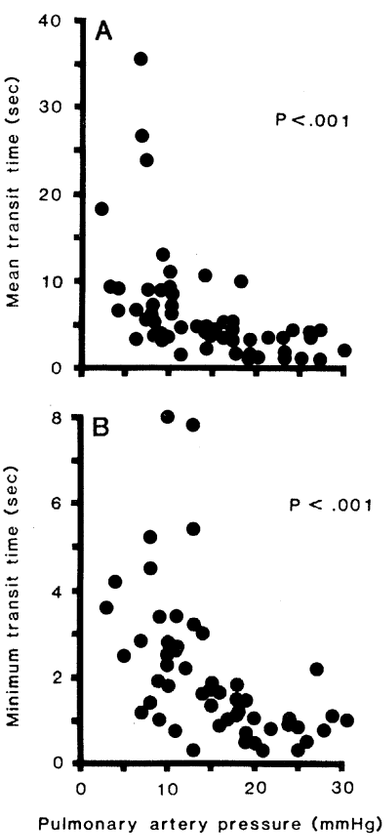

Fig.2. (A) Mean capillary transit times and (B) fastest transit times. Transit times decreased when pulmonary artery pressures were increased by isocapnic airway hypoxia. The average mean capillary transit time for eight dogs under normoxic conditions was 12.7 ± 3.2 seconds at an average pulmonary artery pressure of 7.7 ± 1.0 torr (*11*).

Both the mean and minimum transit times (Fig. 2) were correlated with pulmonary artery pressure ($P < .001$, Spearman's nonparametric ranking test). This relation was predicted by Fung and Sobin in an important theoretical paper (*20*). As expected, very long transit times occurred at low pulmonary artery pressures. As pressure increased, transit times decreased sharply until a pressure of 10 torr was reached. Pressures in excess of 10 torr were accompanied by much smaller decreases in transit times, suggesting an asymptotic approach to the *x*-axis. These data suggest that some mechanism in the pulmonary microcirculation, such as capillary recruitment (*21*), limits red cell velocity and thereby helps ensure complete red cell oxygenation.

Mean transit time was also correlated with cardiac output, so it is not possible to state categorically whether flow or pressure per se controlled transit time in this study. During hypoxia, however, cardiac output increased only 10 percent, whereas pulmonary artery pressure more than doubled and mean capillary transit time decreased by a factor of 4. From the magnitude of these changes it seems likely that pressure is more important than flow in affecting transit time in the upper lung.

WILTZ W. WAGNER, JR.
LEONARD P. LATHAM
MARK N. GILLESPIE
JOHN P. GUENTHER
Cardiovascular Pulmonary Laboratory, University of Colorado Health Sciences Center, Denver 80262
RONALD L. CAPEN
Department of Biology, Colorado College, Colorado Springs 80903

References and Notes

1. F. J. W. Roughton, *Am. J. Physiol.* **43**, 621 (1945).
2. R. L. Johnson, Jr., W. S. Spicer, J. M. Bishop, R. E. Forster, *J. Appl. Physiol.* **15**, 893 (1960).
3. L. B. Rowell, H. L. Taylor, Y. Wang, W. S. Carlson, *ibid.* **19**, 284 (1964).
4. I. H. Young and A. J. Woolcock, *ibid.* **44**, 93 (1978).
5. J. Dempsey, P. Hanson, D. Pegelow, A. Claremont, J. Rankin, *Can. J. Appl. Sport Sci.* **7**, 4 (1982).
6. R. L. Capen, L. P. Latham, W. W. Wagner, Jr., *J. Appl. Physiol.* **50**, 165 (1981).
7. W. W. Wagner, Jr., *ibid.* **26**, 375 (1969).
8. _____, L. P. Latham, R. L. Capen, *ibid.* **47**, 383 (1979).
9. The fluorescein isothiocyanate was tagged to 70,000-dalton dextran (Sigma) to ensure that the dye did not leak out of the microcirculation. The dye was excited at 440 nm; a broad bandpass yellow filter was used as a barrier filter.
10. We placed the catheter 2 to 3 cm proximal to the wedge position so that it would not occupy much of the vessel lumen and impede blood flow to the observed region.
11. Measurement of pulmonary artery pressures are low because the pressure transducer was zeroed at the level of the window (14 cm or 10 torr above the heart).
12. A. Maseri, P. Caldini, S. Permutt, K. L. Zierler, *Circ. Res.* **26**, 527 (1970).

13. T. J. Knopp and J. B. Bassingthwaighte, *J. Appl. Physiol.* **27**, 36 (1969).
14. P. Dow, P. F. Hahn, W. F. Hamilton, *Am. J. Physiol.* **147**, 493 (1946).
15. R. M. Effros, *Circ. Res.* **31**, 590 (1972).
16. K. A. Overholser, J. Bhattacharya, N. C. Staub, *Microvasc. Res.* **23**, 67 (1982).
17. J. B. West, *Ventilation: Blood Flow and Gas Exchange* (Blackwell, Oxford, 1977).
18. P. D. Wagner, *Physiol. Rev.* **57**, 257 (1977).
19. R. L. Conhaim and N. C. Staub, *J. Appl. Physiol.* **48**, 848 (1980).
20. Y. C. Fung and S. S. Sobin, *Circ. Res.* **30**, 470 (1972).
21. Capillary recruitment occurs in the upper lung during hypoxia [W. W. Wagner, Jr., and L. P. Latham, *J. Appl. Physiol.* **39**, 900 (1975)], a change that would slow transit time. Since transit time decreased during hypoxia in this study, capillary blood flow must have increased faster than capillary volume.
22. The authors thank R. F. Grover, J. T. Reeves, and I. F. McMurtry for encouragement and for helpful criticism of the manuscript. A. B. Wagner provided surgical assistance. Supported by NIH grants HL-14985 and HL-07171.

2 June 1982; revised 9 August 1982

Herpes Simplex Virus Type-1 Glycoprotein D Gene: Nucleotide Sequence and Expression in *Escherichia coli*

Abstract. *The protein coding region of the herpes simplex virus type-1 glycoprotein D (gD) gene was mapped, and the nucleotide sequence was determined. The predicted amino acid sequence of the gD polypeptide was found to contain a number of features in common with other virus glycoproteins. Insertion of this protein coding region into a bacterial expressor plasmid enabled synthesis in* Escherichia coli *of an immunoreactive gD-related polypeptide. The potential of this system for preparation of a type-common herpes simplex virus vaccine is discussed.*

The closely related herpes simplex type-1 and type-2 viruses (HSV-1 and HSV-2) are the causative agents of various primary and recurrent human diseases ranging in severity from minor skin infections through often fatal complications (in exposed newborns) and viral encephalitis (*1*). In addition, there may be as many as 9 million cases of recurrent genital infections caused primarily by type-2 each year in the United States alone (*2*).

The infectious HSV particles consist of a linear double-stranded DNA genome of 150 kilobase pairs (kbp) in length contained within an icosahedral nucleocapsid that is in turn surrounded by a membrane envelope (*3*). Embedded within the virion envelope, which is derived from the cellular lipid bilayer during maturation of the virus, are five major HSV-specified glycoproteins, designated gA, gB, gC, gD, and gE (*4*). These virus glycoproteins, with the exception of gA and gB, are antigenically distinct and are required for penetration of the virus into the cell, virus-induced cell fusion, and probably other aspects of virus replication (*5*). Antiserums to each of these glycoproteins can neutralize infectivity of the homologous HSV type in an in vitro assay (*4*, *6*). Whereas antiserums to gC and gE are specific for the HSV type to which they were directed (*6*, *7*), antiserum prepared to HSV-1 gD polypeptide is type-common. Thus, polyvalent gD antiserum (*8*) and certain gD monoclonal antibodies (*9*, *10*) recognize antigenic determinants (epitopes) and neutralize infectivity of both HSV-1 and HSV-2.

The type-common specificity of gD antiserum was demonstrated in vivo by passively immunizing mice with a monoclonal antibody directed against HSV-1 gD (*11*). Such mice were protected against acute neurological disease induced by either HSV-1 or HSV-2. This observation further demonstrated the potential for inducing immunity to infections of both HSV types with the use of a subunit vaccine consisting of a purified HSV-1 gD polypeptide. To this end, we have characterized the genome location and sequence of the HSV-1 DNA encoding gD. Here, we describe the nucleotide sequence of an HSV-1 DNA fragment containing the entire gD polypeptide coding region. Fusion of this coding region with the *lac* promoter enabled synthesis of an immunoreactive gD-related polypeptide in *Escherichia coli*.

The HSV gD gene was mapped by intertypic recombinant analyses (*12*) between 0.9 to 0.945 genome map units (Fig. 1A) in the single-copy short (U_s) region of the virus DNA [for a detailed review of the HSV DNA structure, see (*13*)]. We have mapped the gD gene more precisely by two techniques: (i) by selecting messenger RNA (mRNA) species by hybridization to specific HSV-1 DNA fragments and translation of these mRNA's in vitro and (ii) by expressing cloned HSV-1 DNA fragment by injection into the nuclei of frog oocytes (*14*). We concluded that gD was encoded by a 3.0-kilobase (kb) mRNA, mapping predominantly in a 2.9-kbp Sac I DNA fragment subsequently cloned in plasmid pSC30-4 (Fig. 1B). A recent report by

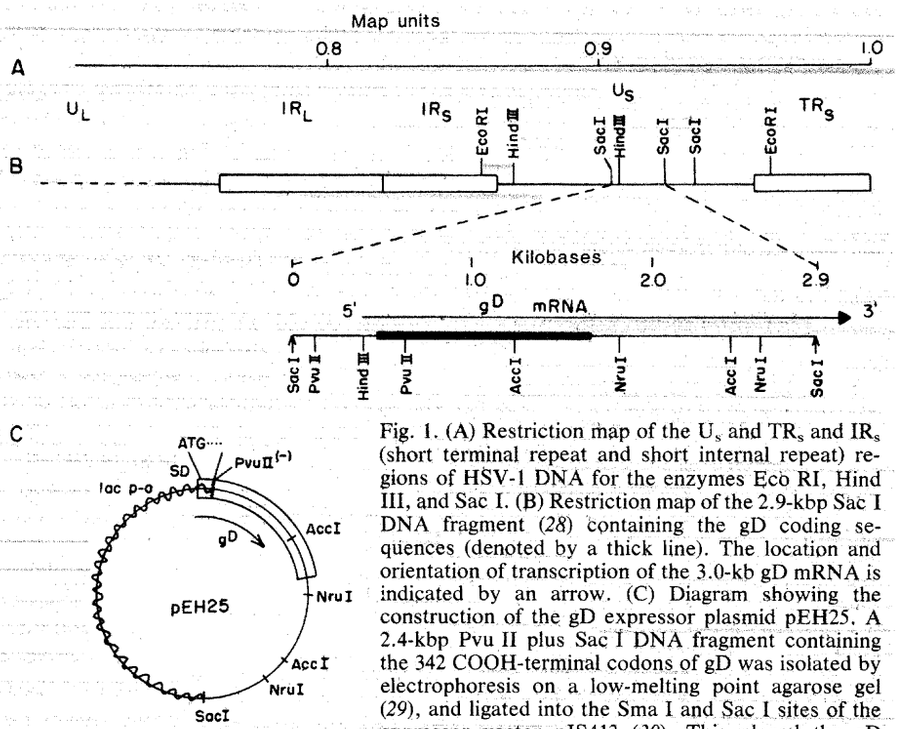

Fig. 1. (A) Restriction map of the U_s and TR_s and IR_s (short terminal repeat and short internal repeat) regions of HSV-1 DNA for the enzymes Eco RI, Hind III, and Sac I. (B) Restriction map of the 2.9-kbp Sac I DNA fragment (*28*) containing the gD coding sequences (denoted by a thick line). The location and orientation of transcription of the 3.0-kb gD mRNA is indicated by an arrow. (C) Diagram showing the construction of the gD expressor plasmid pEH25. A 2.4-kbp Pvu II plus Sac I DNA fragment containing the 342 COOH-terminal codons of gD was isolated by electrophoresis on a low-melting point agarose gel (*29*), and ligated into the Sma I and Sac I sites of the expressor vector pJS413 (*30*). This placed the gD coding region in the correct reading frame downstream from a modified λ *cro* sequence (*26*) containing the Shine and Dalgarno sequence (*SD*), the initiation sequence (*ATG*), and a further 23 codons. HSV-1 DNA sequences are represented by a smooth circular line and those derived from pJS413 by a wavy line. These coding sequences (indicated by an open circular box) are transcribed in the direction indicated by the arrow under the control of the *E. coli lac* promoter (*lac p-o*). This plasmid, pEH25, was used to transform *E. coli* strain NF1829 (*31*).

0036-8075/82/1022-0381$01.00/0